



3D fractal DNA assembly from coding, geometry and protection

ALESSANDRA CARBONE^{1,*}, CHENGDE MAO², PAMELA E. CONSTANTINOU³, BAOQUAN DING³, JENS KOPATSCH³, WILLIAM B. SHERMAN³ and NADRIAN C. SEEMAN³

¹*Department of Computer Science and Laboratory of Analytical Genomics, INSERM U511, Université Pierre et Marie Curie 91, Boulevard de l'Hôpital, 75013 Paris, France* (*Author for correspondence, e-mail: carbone@ihes.fr); ²*Department of Chemistry, Purdue University, West Lafayette, IN 47907-1393, USA;* ³*Department of Chemistry, New York University, New York, NY 10003, USA;*

Abstract. We present DNA components whose 3D geometry and cohesive portions are compatible with a fractal 3D assembly. DNA parallelograms have been proposed in Carbone and Seeman [(2002b) *Natural Computing* 1: 469–480; (2003) *Natural Computing* 2: 133–151] as suitable building blocks for a 2D fractal assembly of the Sierpinski carpet. Here we use Mao 3D triangles, which are 3D geometrically trigonal molecules, to construct basic building blocks and we obtain a simplified version of the 2D assembly design. As in the previous 2D construction, we utilize the interplay of coding in the form of cohesive ends, geometrical complementarity and protection of potentially undesirable sites of reactivity. The schema we propose works for trigonal symmetries and the Mao triangle is one example of a possible DNA trigonal tile.

Key words: coding of times, DNA 3D assembly, DNA molecules, DNA protection, DNA nanotechnology, geometry of tiles, Sierpinski cube, tiling

1. Introduction to 3D fractals and background

We present a scheme whereby we can build a set of patterns based on rhombohedra through a fractal process of assembly. The 2-dimensional form of the Sierpinski carpet studied in Carbone and Seeman (2002, 2003) is here generalized to 3D. The rhombus used previously is here generalized to its 3D analog, a rhombohedron.

The Sierpinski cube fractal, also called Menger sponge or Sierpinski sponge, is illustrated in Figure 1. This pattern can be constructed in two ways. The first method starts with a solid (filled) cube, divides it into 27 smaller congruent cubes, and removes the interior of the cube as well as the middle cubes on its six faces. This sequence of steps is then applied

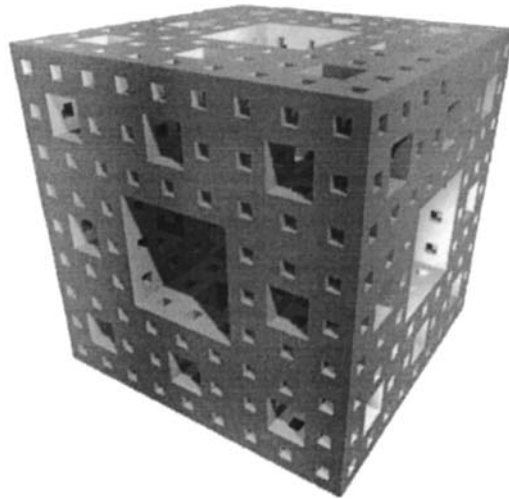


Figure 1. A Sierpinski cube fractal. This drawing illustrates the results of four iterations of a fractal process described in the text.

again to each one of the 20 remaining cubes which will be divided in 27 smaller congruent cubes, and so on. The construction can be repeated infinitely often and Figure 1 illustrates the result of the procedure after four iterations. The second method, exploits the rational symmetry of a cube: The idea is to take a cube, scale it by a factor of $1/3$ and translate 20 copies of it in some appropriate way, so as to form a cube with a “hole” in the middle and a “hole” in the middle of each one of its faces. This new (symmetric) shape is duplicated, then scaled, and translated again. The procedure can be repeated infinitely often and the result is the Sierpinski cube fractal. Again, four iterations of this procedure produce Figure 1. The Sierpinski cube attracts attention because of its geometrical properties: the area $A(0) = 24$, $A(n) = (8/9)^n \cdot 16 + (20/9)^n \cdot 8$ grows to infinity with the number of iterations n , while the volume $V(0) = 8$, $V(n) = (20/27)^n \cdot 8$ goes to 0 as n approaches infinity.

We wish to construct an analog of the Sierpinski cube fractal with DNA tiles. The idea of the construction follows the second method. There will be no scaling in our case, and the construction of the repeated pattern is illustrated in Figure 2 for a simple cube. There are two kinds of cubes which are used as basic building blocks, one labeled a, b, c and the other labeled with complementary labels a^*, b^*, c^* . Opposite faces in the cube are labeled the same way. By using a single cube, one would not be able to glue together two distinct cubes, since no complementary labels would exist. By using two kinds of cubes, one encounters prob-

lems of ambiguity during self-assembly and undesirable shapes might be constructed. For instance, pairs of distinct cubes might glue on the opposite faces of a third cube and allow for the construction of chains of cubes or of cross-shaped structures. To avoid these kinds of shapes we introduce a different geometry for opposite faces of the cubes, but the idea explained above remains the same.

2. Motivation to go to 3D

It is key to our understanding of the properties of matter that we be able to extend any “(self-)assembly capabilities” existing in one or two dimensions to a three-dimensional context, that is the world where we live. Here, we seek to extend the systems we have proposed previously in two dimensions to three dimensions. We seek to construct the three-dimensional fractal system described here by the methods of structural DNA nanotechnology. The goals of structural DNA nanotechnology are to obtain the greatest possible control over the structure of matter in three dimensions. In addition to periodic systems, the construction of aperiodic arrays is key to this level of control. Pseudocrystalline arrangements are central to DNA, from genetics (Schrödinger, 1944) to nanotechnology (Carbone and Seeman, 2002a; Seeman, 2003), and fractal constructions are among the simpler systems to envision. The ability to construct fractals impinges on the ability to do aperiodic assembly in 3D. The extent to which this is possible will likely dictate the extent to which 3D self-assembly methods can be used for molecular computation. Likewise, fractal materials are likely to be of the greatest value when they are constructed in 3D. For example, fractal materials such as the ones described here may well facilitate the cooling of nanoelectronic circuitry more effectively than continuously periodic crystalline systems.

3. The specific DNA molecular system proposed

The formation of any well-defined array requires well-structured building blocks. Here, we have selected the Mao 3D triangle as the basis for our system. This is a trigonal arrangement of three Holliday (1964) junction-like motifs in an interwoven fashion, as illustrated in Figure 3. The Holliday junction contains four strands arranged into four double helical arms that flank a branch point. Previously, we have reported rigid double crossover (DX) structures containing two Holliday junc-

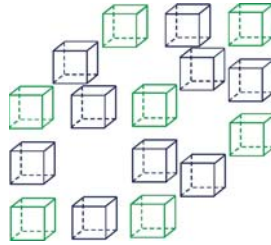
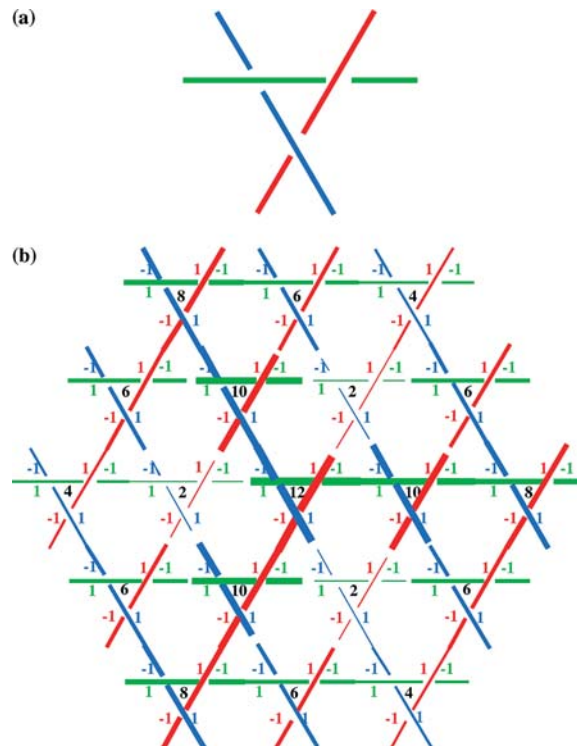


Figure 2. Assembly of a Sierpinski cube or rhombohedron. There are two kinds of basic building blocks represented as green and blue rhombohedrons. They are used to build the corners and the edges of the rhombohedron.

tions (Fu and Seeman, 1993), and well-structured parallelograms built from four Holliday junctions (Mao et al., 1999). The 3D triangle is intermediate between these systems, containing three Holliday junctions. It is key to all of these structures that the Holliday junction is known to stack its four arms in a pairwise fashion (Churchill et al., 1988). Thus, there are two domains, usually forming an angle of about 60° between them (Mao et al., 1999), although other angles are known



(Eichmann et al., 2000; Sha et al., 2000, 2002). The DX molecule severely distorts the angle between stacked Holliday junction domains so that the domains are parallel or antiparallel. By contrast, the angle seems unperturbed in both the DNA parallelogram and in the 3D Mao triangle. The DNA helical domains make an angle with the trigonal axis of the system. This angle is clearly a function of the separation of the vertices. As they separate, the angle of (unrealistically) rigid domains would approach 90° in the limit of infinite separation. It is important to recognize that there are two possible signs for the Mao triangle. Using about 16–17 nucleotide pairs between junctions (slightly over a one and a half turns) leads to a ‘positive’ molecule (Figure 3a). However, using about 14 nucleotide pairs between junctions leads to a ‘negative’ molecule, whose helix axes are organized so that the chirality of their interweaving is of the opposite sign; i.e., the helix axis organization looks roughly like the mirror image of the positive molecule. Both the positive and the negative molecules crystallize (CM, PEC, JK and NCS, unpublished), but the crystals of the negative form do not diffract well. It should be clear that the structural characteristics of the DNA double helix (20 Å diameter and 10.5 nucleotide pairs per turn) limit the possible separations of vertices to discrete values.

It is possible to arrange eight parallel Mao 3D triangles at the corners of a rhombohedron, with the help of 12 other Mao 3D triangles acting as the edges of the rhombohedron. This rhombohedron is the basis of our proposed fractal assembly. The rigidity of this rhombohedron is difficult to estimate at this time. However, a rhombohedral crystalline lattice self-assembled from 3D triangles has been shown to be ordered to a resolution of ~ 1 nm (CM, PEC and NCS, unpublished).



Figure 3. A Sierpinski–Mao rhombohedron. The Sierpinski–Mao rhombohedron is defined by assembly of 20 copies of Mao triangular molecule. An individual Mao triangular molecule is shown schematically in (a). The triangle used in the figure has positive sign and the assembly properties are indicated by the coloring of the edges of the triangles. To help the reader to keep track of the three dimensions, we have labeled the centers of each triangle with a number: two triangles have same value when they lie on the same plane. Value 12 corresponds to the plane which is closest to the eye of the observer. A total of seven planes realize the entire rhombohedron. For clarity, the bottom triangle (with value 0) is not drawn. Note that gaps are shown when the numbers of the triangles flanking the gap differ by more than 2. Each corner of the rhombohedron is constituted either by three corner faces of obtuse angle or by two corner faces of acute angle and one corner face of obtuse angle. The 3-dimensionality of the construction is represented by the thickness of the sides of the rhombohedron: thicker Mao triangular molecules are closer to the reader than thin Mao triangles.

More robust molecules can be built if each double helical edge of the Mao triangle is replaced by double crossover (DX) molecules; DX molecules are about twice as stiff as linear DNA (Sa-Ardyen et al., 2003a). We propose to make eight different variants of the rhombohedron. The three helix axes do not meet at right angles. Therefore, we must deal with a rhombohedron of trigonal symmetry, rather than a cube of octahedral symmetry. The main consequence of this is that we cannot use rotated versions of our units to produce elements in our fractal construction, and ultimately must make eight rhombohedra whose edges are either DNA double helices, or DNA double crossover molecules.

4. The Sierpinski cube made from Mao molecules

The basic building block of the fractal construction is the *Sierpinski–Mao rhombohedron*. This molecule is constructed by the assembly of 20 Mao triangles following the schema illustrated in Figure 3. Shown in that figure are 19 3D triangles. Their elevations range from 2 to 12, with a 20th one (at level 0) occluded by the one at the 12th level in the center. Each edge of each triangle has a positive side (denoted by +1) and a negative side, denoted by -1. Connections are indicated by continuous red, blue or green lines. Clearly 7 of the triangles that would fill a $3 \times 3 \times 3$ volume are missing. These are the ones in the centers of each face, and the one at the center of the entire polyhedron. External features of the rhombohedron, such as long and short extensions (see discussion below), are not indicated in Figure 3. Individual rhombohedra, such as the one shown in Figure 3 should be possible to assemble by the methods used previously to build a cube (Chen and Seeman, 1991), a truncated octahedron (Zhang and Seeman, 1994), and an arbitrary graph molecule (Sa-Ardyen et al., 2003b).

In the assembly of the Sierpinski–Mao cube we only use one of the two possible kinds of Mao triangles, say the one with positive sign, but the one with negative sign would work as well to build the basic building blocks. Likewise, we could use the Mao triangle containing DX molecules. Insofar as we can tell, the DX Mao triangle is much more robust than the one built from simple linear duplex. For example, it is capable of forming 2D arrays, such as the one shown in Figure 4. The rhombohedron that we propose is a 3-connected object, much like the DNA cube we built previously (Chen and Seeman, 1991). However, the new rhombohedra will be able to link among themselves along each of their

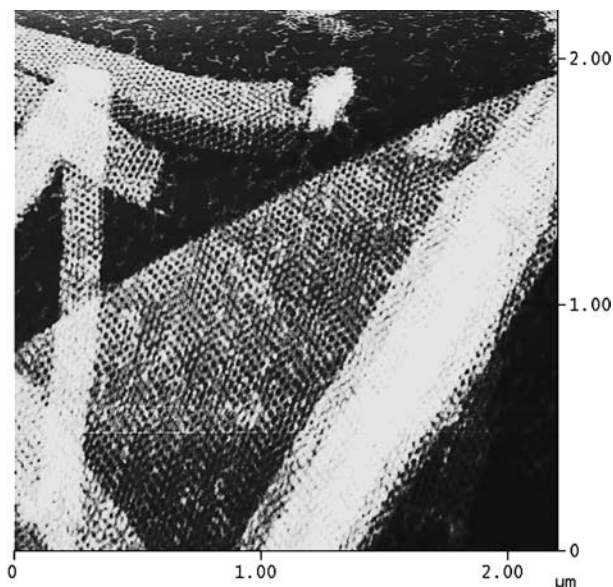


Figure 4. A 2D array generated from DX-based Mao triangles. This is an atomic force micrograph of a 2D array whose components are Mao triangles. The array was created by blunting the sticky ends in one direction, so that only two dimensions of propagation are possible. Note the regular arrangement of the repeating units. The pink area is folded over the other portion of the array.

edges, whereas the old DNA cube was unable to interact with other molecules.

Each face of a Sierpinski–Mao rhombohedron is characterized by four extensions. Each edge of a face corresponds to two of such extensions, one for each extreme. Two consecutive edges share one extension, since they share an extreme. Extensions are of two sorts, long and short. In practice this means that a long extension is a helix of, say three turns, while a short one is a helix of about two turns. Each face has two long extensions and two short ones. The persistence length of double stranded DNA under standard conditions is about 15 turns (Hagerman, 1988), and that of the DX is about twice as long (Sa-Ardyen et al., 2003a, b), so extensions of these sizes are expected to behave quite rigidly. In all, a Sierpinski–Mao cube has 24 extensions, 4 for each face, 12 long and 12 short. We ignore the middle extensions on the Mao triangles; we specify that they are blunt-ended and too short to interact with another cube; therefore, they do not contribute to the intermolecular interactions.

5. The eight varieties of the Sierpinski–Mao rhombohedron

There are eight different kinds of Sierpinski–Mao rhombohedra that we use. They are characterized by different labels and geometry of the faces. The first, called T , is illustrated in Figure 5 (top, left). It has three kinds of labels a , b , c which correspond to the three edge directions of the rhombohedron. One of the corners of the rhombohedron is made by long branches only; its three adjacent corners are made by two long branches and one short branch; the three next adjacent corners are made of two short branches and one long one, and finally the remaining corner (lying on the diagonal of the rhombohedron coming from the first corner we considered) has three short branches. There are three other kinds of rhombohedron with labels a , b , c ; these are shown in Figure 5 as T^2x , T^2y and T^2z . The superscript ‘2’ indicates that we have reversed the extensions in two directions; were the rhombohedron a cube, these reversals would correspond to rotations of the T tile about the x , y or z axes, as indicated (see Figure 5). If one draws correspondences between the a , b and c directions with x , y and z directions, respectively, then these variants on T are logically equivalent to rotations such that the unaltered extensions lie in planes normal to the designated direction. If the rhombohedron were a cube, they could be generated from T by 180° rotations, but that is not possible with a rhombohedron. The positions of two sets of extensions are changed from T in these variants. For example, T^2x exchanges the long and short extensions on the a and b directions, while not changing the plane perpendicular to a .

The other four rhombohedra are called $T^{*1}x$, $T^{*1}y$, $T^{*1}z$ and T^{*3} . The first three have a single pair (hence the superscript ‘1’) of extension planes exchanged, through either the x , y or z direction of the T tile; this has the effect that the c faces in $T^{*1}x$, which are orthogonal to the x axis (in an ideally cubic tile), have extensions whose sizes are different than in the c faces of T ; the a faces in $T^{*1}y$, ‘orthogonal’ to the y axis, and the b faces in $T^{*1}z$, orthogonal to the z axis, changed in a similar manner. The rhombohedron T^{*3} has all three sets of planes exchanged, with the effect that all faces exchanged the sizes of the extensions. The ‘*’ in their designations indicates that the sticky ends on the ends of their extensions are the complements to those on the first set. With this notion in mind, the differences between the ‘*’ and non-‘*’ components are evident from Figure 5.

In physical terms, we say that a face is *labeled* a when the sticky-ends of its four extensions are labeled by the same sequence, such as a . The

same extends to labeling the other faces. The labels a, a^*, b, b^* , and c, c^* are pairwise complementary. We say that a face of the rhombohedron *complements* a face of another rhombohedron when the two faces are labeled by complementary labels and when the four extensions situated face-to-face are pairwise complementary in length, i.e. a short extension opposes a long one and vice versa. Two faces bind one another when they are complementary and their opposite sticky-ends pairwise bind to each other. The faces of all eight rhombohedra always contain two long extensions and two short ones. In particular, the two long extensions are always adjacent to each other and this makes the binding of two complementary faces unambiguous.

6. Assembly of fractal layers

Let $T, T^2x, T^2y, T^2z, T^{*1}x, T^{*1}y, T^{*1}z$ and T^{*3} be building blocks constituting layer 0 and let $T', T^2x', T^2y', T^2z', T^{*1}x', T^{*1}y', T^{*1}z'$ and $T^{*3'}$ be the eight rhombohedra that one wants to construct out of the assembly of suitable copies of the 0-layer components. The rhombohedra $T', T^2x', T^2y', T^2z', T^{*1}x', T^{*1}y', T^{*1}z'$ and $T^{*3'}$ form layer 1. These eight rhombohedra are illustrated in Figure 6a–h. Note that the faces of T', T^2x', T^2y', T^2z' are labeled by triplets aa^*a, bb^*b, cc^*c coding for the edges of the faces, and that the faces of $T^{*1}x', T^{*1}y', T^{*1}z'$ and $T^{*3'}$ are labeled with triplets $a^*aa^*, b^*bb^*, c^*cc^*$. The geometry of the faces of rhombohedron T' follows the geometry of the faces of rhombohedron T ; namely, if an edge of a face of T is constituted by two extensions which are, say long–short, then the corresponding edge in T' is constituted by a sequence of six extensions long–short–long–short–long–short. The same holds for any edge geometry of T , and also for all other rhombohedra.

Figure 6 illustrates the assembly of all of the first-layer rhombohedra. The 0-layer rhombohedron lies at each of the eight corners, four complementary (starred if the rhombohedron is unstarred, and unstarred if the rhombohedron is starred) rhombohedra encircle the system as belts in each of the three directions. For example T' consists of T at each of the corners, its upper and lower copies held together by four $T^{*1}z$ rhombohedra, its front and back copies held together by four $T^{*1}x$ rhombohedra, and its left and right copies held together by four $T^{*1}y$ rhombohedra. In a similar vein, $T^{*1}z'$ consists of eight $T^{*1}z$ rhombohedra at each corner, its upper and lower copies

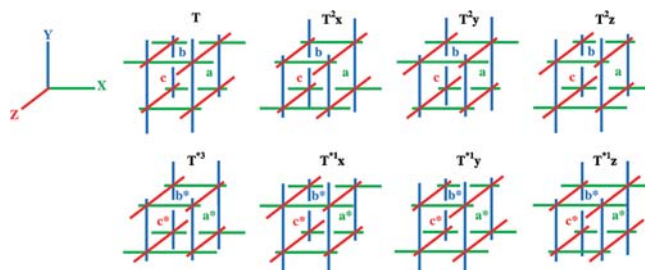


Figure 5. The eight different fractal 0-layer rhombohedral components in this system. The eight components described in the text are shown. The T rhombohedral component is the reference molecule, and its edges terminate in sticky ends a , b or c . The T^2x , T^2y and T^2z components also terminate in a , b or c , but two of their edges have been switched, so that the long and the short extensions are now on opposite sides of the rhombohedron. Were the component a cube, these components would be unnecessary. The $T^{*1}x$, $T^{*1}y$, $T^{*1}z$ and T^{*3} components all end in a^* , b^* or c^* , the complements of a , b or c . All three extensions have been switched in T^{*3} , but only a single set of extension has been switched in $T^{*1}x$, $T^{*1}y$ or $T^{*1}z$. For clarity, the rhombohedra are drawn somewhat like cubes. A coordinate system is indicated on the left.

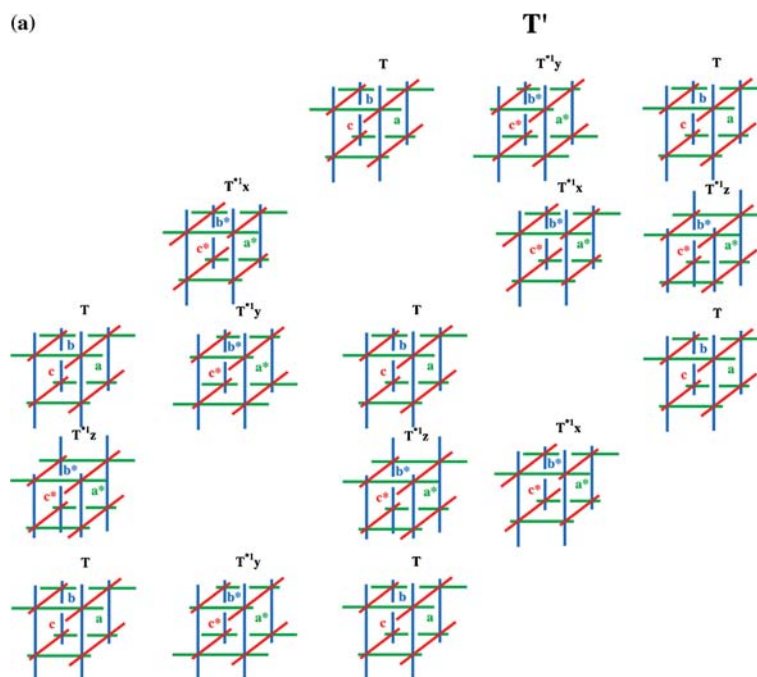


Figure 6(a-h). The eight 1-layer fractal rhombohedra. Each of the rhombohedra are shown in an exploded view, so that the edges holding them together can be identified. For clarity, only the front, right and top faces are shown, so only seven corner rhombohedra and three rhombohedra from the middles of the edges are visible for each of the three types. One corner rhombohedron and three edge-middle rhombohedra are missing, and sixteen are shown.

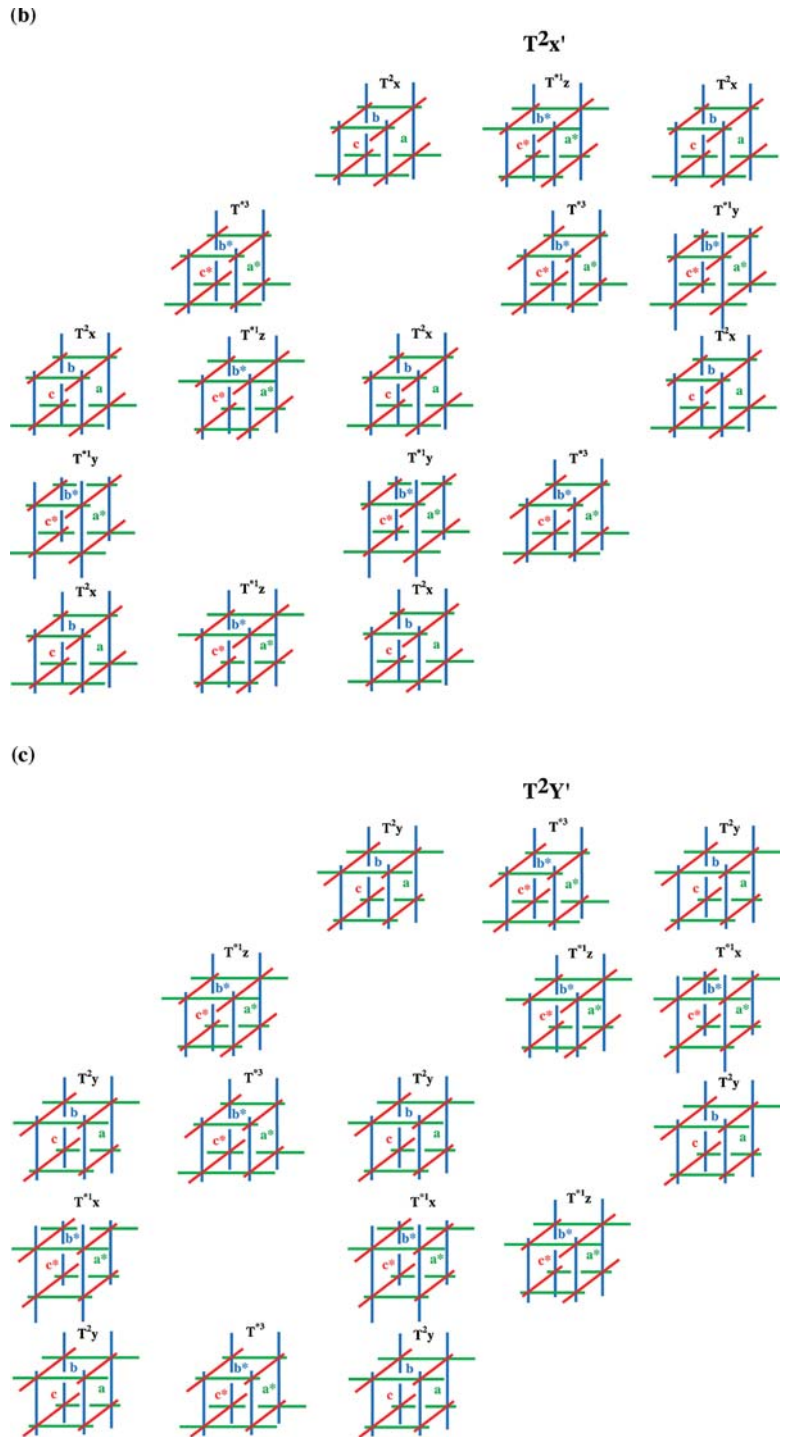


Figure 6. (Continued)

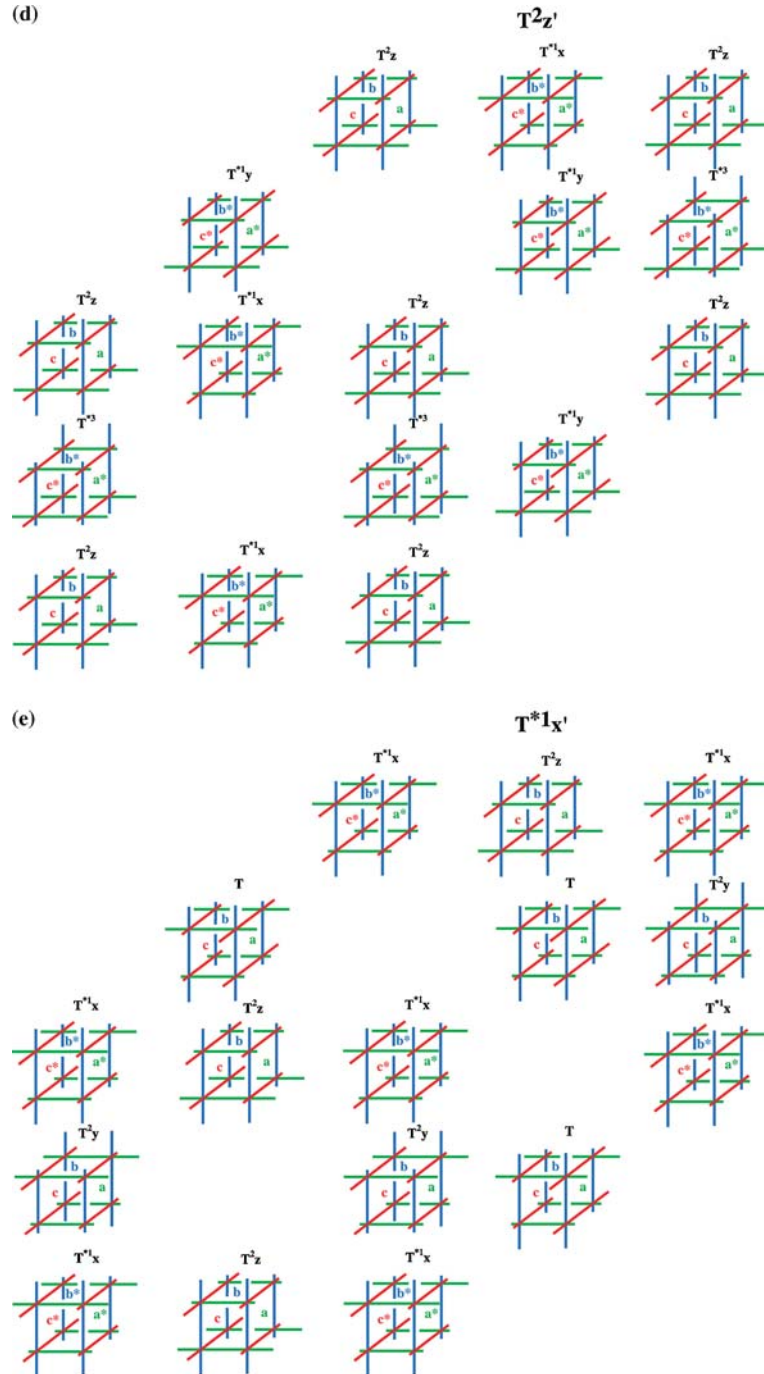


Figure 6. (Continued)

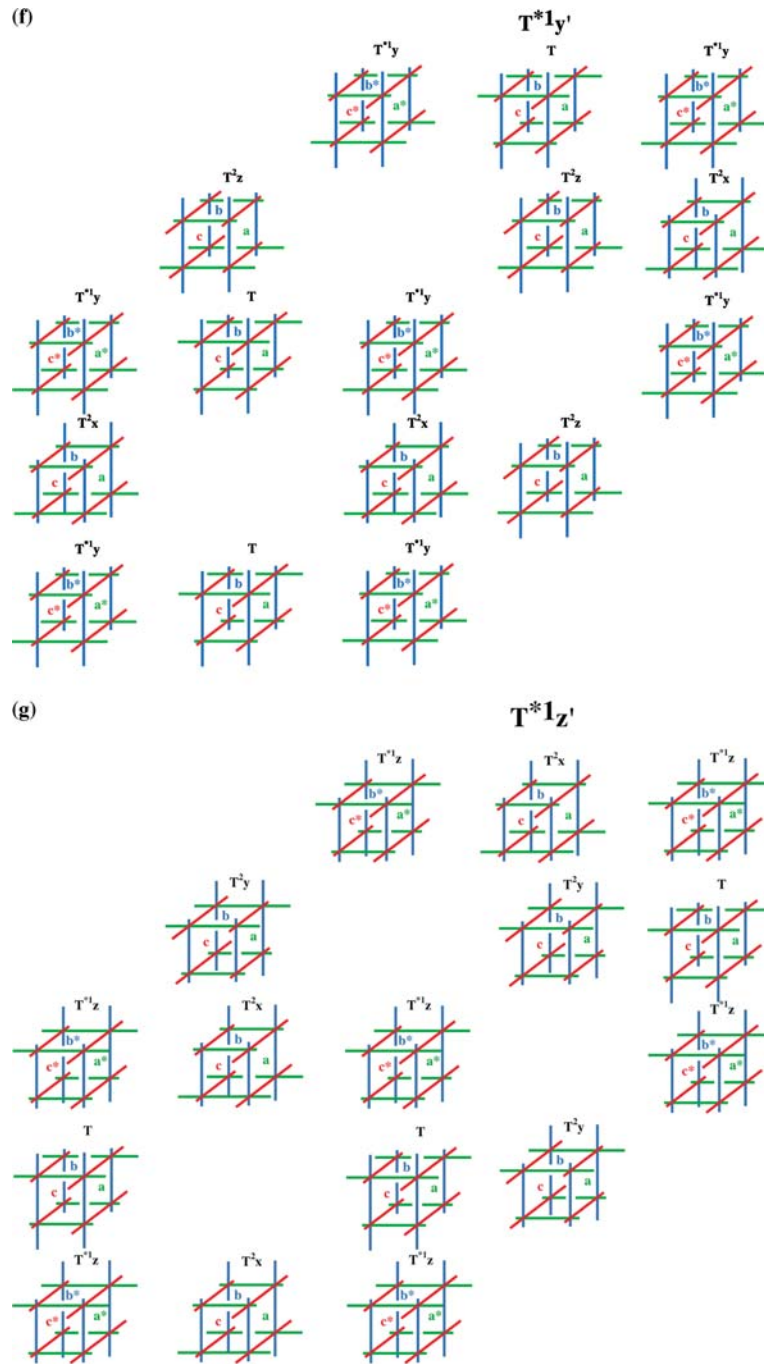


Figure 6. (Continued)

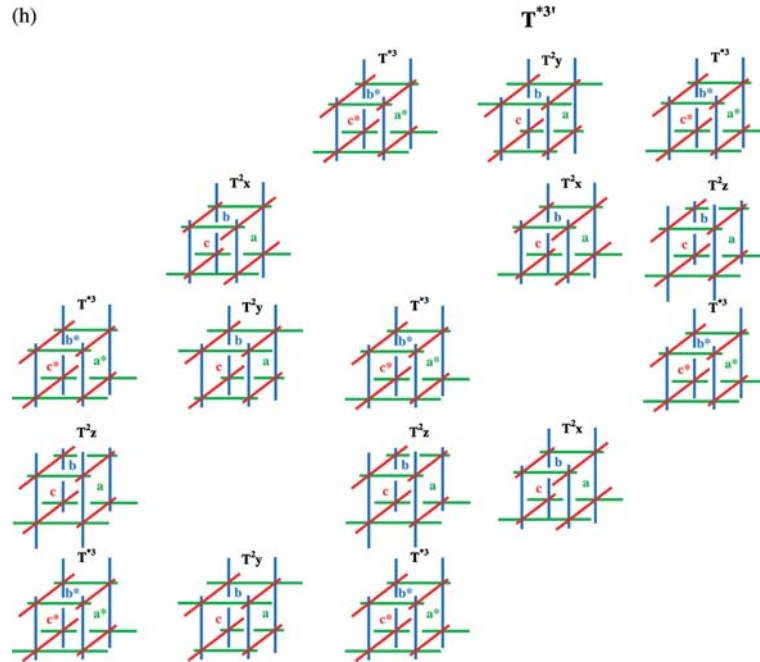


Figure 6. (Continued)

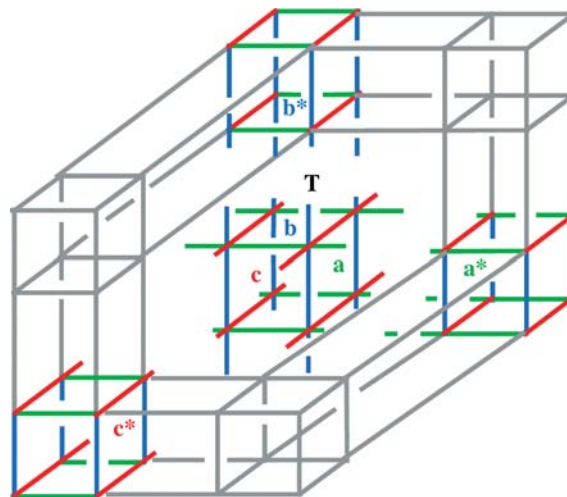


Figure 7. Corner protection. The T rhombohedron closest to the reader in Figure 6a is shown protected by a collection of 3 rhombohedra with edges (derived from the initial rhombohedra in Figure 5) and three others drawn in gray, just to indicate that they are connected. This is an exploded view. A possible fourth gray rhombohedron is omitted for clarity; it would be directly in front of the protected T tile. The faces labeled a and a^* , b and b^* , c and c^* are supposed to glue together. All other faces remain free for binding.

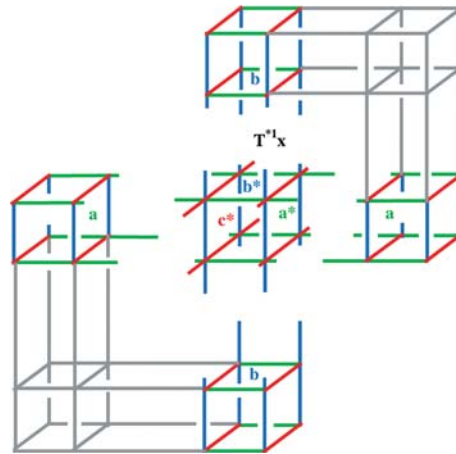


Figure 8. Edge protection. Here, the $T^{-1}x$ rhombohedron from Figure 6a is shown protected by four flanking rhombohedra divided into two 'L' or 'V'-shaped units of two rhombohedra each. This is an exploded view. In fact, these rhombohedra would need to be less than half as thick as the original tiles so that more than one could be used simultaneously. This requirement should be relatively easy to achieve, however, so it is not an obstacle to the construction.

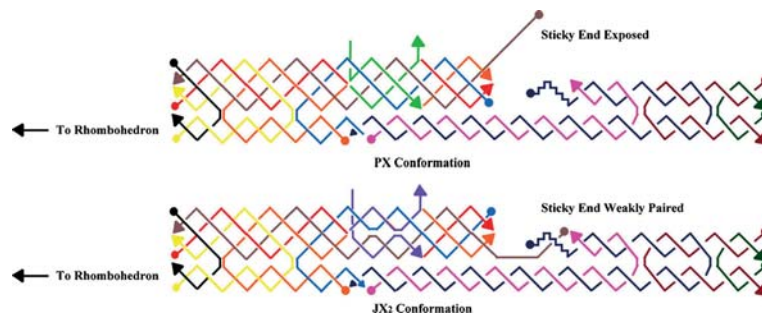


Figure 9. An alternative form of protection for the sticky ends. These schematic diagrams contain a PX-JX₂ device (Yan et al., 2002) attached to a 3-domain unit. The device is shown in both of its states, the PX conformation in the upper diagram and the JX₂ conformation in the lower diagram. The states of the devices are established by the green set strands (upper diagram) or the purple set strands (lower diagram). The bottom domain is bonded on the left to the rhombohedron, as noted. It is hybridized with a protecting unit on the right; light and dark blue strands hybridize to join this protecting unit to the bottom domain. The protecting unit can be removed by standard Yurke-style (2000) techniques. When the device is in the PX state, the brown strand with the sticky end is available for hydrogen bonding with another rhombohedron unit (not shown). However, when it is in the JX₂ conformation, the position of the sticky end has been shifted by about 4 nm. In this position it is unavailable for hydrogen bonding with another rhombohedron. In addition, it is tied up weakly with a partially mispaired sticky end (dark blue) from the protecting unit. In the presence of its true complement, the mispaired sticky end can be competed away, freeing the brown sticky end to have its position reversed when the device changes from the JX₂ state to the PX state.

held together by four T rhombohedra, its front and back copies held together by four T^2_y rhombohedra, and its left and right copies held together by four T^2_x rhombohedra.

Each of the corner rhombohedra must be protected on the three faces that are designated not to be reactive. The easiest way to do this is by using a 6-rhombohedron or 7-rhombohedron unit complementary to the outer faces. An example of a 6-rhombohedron unit protecting the right-top-front corner rhombohedron T in T' is shown in Figure 7. A seventh rhombohedron could be added to connect the three gray rhombohedra above the T rhombohedron shown. There need to be four different geometrical types of corner cubes, two for the vertices flanking the three-fold axis of the rhombohedron (covering three obtuse angles of the rhombohedron) and two others for the six vertices in between (containing two acute and one obtuse angles). The top vertex has a protectable surface enantiomorphic to the bottom vertex, and the outer surfaces of the top three are also enantiomorphic to the bottom three. Within this context, we expect that the generalized protection procedures introduced earlier (Carbone and Seeman, 2003) should be effective here, as well. These protections are necessary to allow for selective removal of labels belonging to different tiles, after the assembly of several building blocks is realized.

We must also protect the central rhombohedra in each edge, to ensure that they are not capable of incorrect pairing. An example of this type of protection using two components is illustrated in Figure 8. Each of the three central rhombohedra requires two such components, so there are six protecting groups needed to assemble each of the first-layer rhombohedra illustrated in Figure 6, leading to 48 protecting groups in all. It is clear that we have taken artistic license in this drawing both for clarity, to indicate the connection between the original rhombohedra and the protecting groups. As a practical matter, the height and width of the protecting unit (drawn as eight rhombohedra) must be less than twice the width of the central rhombohedron, or two such protected units cannot be used simultaneously in the same layer. If the protecting groups can be made according to this prescription, all of the 20 rhombohedra could be put together in solution so that they could self-assemble into the desired fractal molecule. Removal of the protecting groups would be done as suggested earlier, using Yurke et al. (2000) techniques. Higher fractal units and their protecting groups would be constructed in a fashion similar to those for the lower layers.

7. Concluding remarks

We have demonstrated here that it is possible to extend fractal assembly of DNA components from two dimensions to three dimensions. We have shown that a trigonally symmetric 3D tile, the rhombohedron, can be used as the basis of this assembly. We propose constructing our rhombohedra from Mao DNA triangles. These triangles come in two different ‘enantiomers’, with either a positive or negative angle between the helices. As a practical matter, these triangles are much better behaved when constructed not from individual triangles, but from DNA DX molecules. Thus, the individual helices we have schematized in this paper might well be represented best by fused double helices. We are optimistic that within a few years the structures proposed here will be made in the laboratory, so that aperiodic assembly is extended to three dimensions.

The high number of protection shapes that one needs for the construction leads us to propose an alternative to the exhaustive combinatorial solution. The notion is to replace the simple ends of bonding points in a Mao-triangle with a protected PX–JX₂ device (Yan et al., 2002), as shown in Figure 9. To protect a sticky end, we switch it from PX to JX₂. When in the PX state, the end (a,b,c,a^*,b^*,c^*) is free. When in the JX₂ state, it is bound up weakly. A protected and an unprotected molecule are both bound by a protecting group, which is on the right side of the drawing. Its long domain is drawn in dark blue and violet. When the device is in the JX₂ state, the dark blue end pairs with the active sticky end, but weakly, just to tie it down. This notion of generalized protection allows us to avoid the large combinatorics of shapes and coding by eliminating the shape requirement from the protecting groups and letting only the coding play a role. However, it requires to distinguish between pairs of faces coded in the same manner in a rhombohedron. Such a distinction allows us to simulate by coding the shape requirement and prevent only triplets/pairs of faces sharing the same corner/edge to be protected. Isolation of individual components during the protection-group addition process can help to simplify this process, as it did in the 2D case (Carbone and Seeman, 2003); thus, a stepwise method is likely to have an advantage over a single-pot reaction.

References

- Carbone A and Seeman NC (2002b) A route to fractal DNA assembly. *Natural Computing* 1: 469–480

- Carbone A and Seeman NC (2002a) Circuits and programmable self-assembling DNA structures. *Proceeding of the National Academic Sciences (USA)* 99: 12577–12582
- Carbone A and Seeman NC (2003) Coding and geometrical shapes in nanostructures: A fractal DNA-assembly. *Natural Computing* 2: 133–151
- Chen J and Seeman NC (1991) The synthesis from DNA of a molecule with the connectivity of a cube. *Nature* 350: 631–633
- Churchill MEA, Tullius TD, Kallenbach NR and Seeman NC (1988) A Holliday recombination intermediate is twofold symmetric. *Proceedings of the National Academic of Science (USA)* 85: 4653–4656
- Eichman BF, Vargason JM, Mooers BHM and Ho PS (2000) The Holliday junction in an inverted repeat DNA sequence: sequence effects on the structure of four-way junctions. *Proceedings of the National Academic Science USA* 97: 3971–3976
- Fu T-J and Seeman NC (1993) DNA double crossover structures. *Biochemistry* 32: 3211–3220 (1993)
- Hagerman PJ (1988) Flexibility of DNA. *Annual Review in Biophysics and Biophysical Chemistry* 17: 265–286
- Holliday R (1964) A mechanism for gene conversion in fungi. *Genetics and Research* 5: 282–304
- Mao C, Sun W and Seeman NC (1999) Designed two-dimensional DNA Holliday junction arrays visualized by atomic force microscopy. *Journal of the American Chemical Society* 121: 5437–5443
- Mao C, LaBean T, Reif JH and Seeman NC (2000) Logical computation using algorithmic self-assembly of DNA triple crossover molecules. *Nature* 407: 493–496
- Sa-Ardyen P, Vologodskii AV and Seeman NC (2003a) The flexibility of DNA double crossover molecules. *Biophysics Journal* 84: 3829–3837
- Sa-Ardyen P, Jonoska N and Seeman NC (2003b) Self-assembling DNA graphs. In: *DNA-Based Computers VIII*, LNCS 2568, pp. 1–9. Springer-Verlag, Berlin
- Schrödinger E (1944) *What is Life? and Mind & Matter*. Cambridge University Press, London (republished, 1967)
- Seeman NC (2003) DNA in a material world. *Nature* 421: 33–37
- Sha R, Liu F, Millar DP and Seeman NC (2000) Atomic force microscopy of parallel DNA branched junction arrays. *Chemistry and Biology* 7: 743–751
- Sha R, Liu F and Seeman NC (2002) Atomic force measurement of the inter-domain angle in symmetric Holliday junctions. *Biochemistry* 41: 5950–5955
- Yan H, Zhang X, Shen Z and Seeman NC (2002) A robust DNA mechanical device controlled by hybridization topology. *Nature* 415: 62–65
- Yurke B, Turberfield AJ, Mills AP Jr., Simmel FC and Neumann JL (2000) A DNA-fueled molecular machine made of DNA. *Nature* 406: 605–608
- Zhang Y and Seeman NC (1994) The construction of a DNA truncated octahedron. *Journal of the American Chemical Society* 116: 1661–1669